Available online at www.sciencedirect.com
SCIENCE DIRECT
Solid State Communications 136 (2005) 16–21
solid state communications
www.elsevier.com/locate/ssc

High pressure behaviour of $KHSO_4$ studied by electrical impedance spectroscopy

N. Bagdassarov[a,*], G. Lentz[b]

[a]*Arbeitsbereich Geophysik, Universität Frankfurt, Felbergstraße 47, D-60323 Frankfurt am Main, Germany*
[b]*Mineralogisch-Petrographisches Institut und Museum, Universität Kiel, D-24098 Kiel, Germany*

Received 3 May 2005; received in revised form 22 June 2005; accepted 23 June 2005 by A.K. Sood
Available online 11 July 2005

Abstract

Measurements of the electrical conductivity were performed in $KHSO_4$ at pressures between 0.5 and 2.5 GPa and in the temperature range 120–350 °C by the use of the impedance spectroscopy. The temperatures of the α–β phase transition (T_{Tr}) and of the melting (T_m), determined from the Arrhenius plots $\ln(\sigma T)$ vs. $1/T$, increase with pressure up to 1.5 GPa having $dT/dP \sim +45$ K/GPa. Above the pressure 1.5 GPa, the pressure dependencies of T_{Tr} and T_m are negative $dT/dP \sim -45$ K/GPa. At pressures above 0.5 GPa, the reversible decomposition of $KHSO_4$ into $K_3H(SO_4)_2 + H_2SO_4$ (and probably into $K_5H_3(SO_4)_4 + H_2SO_4$) affects the electrical conductivity of $KHSO_4$, with the typical values of the protonic electrical conductivity, *c*. 10^{-1} S/cm at 2.5 GPa.

PACS: 84.37; 74.25.F; 84.32.F; 82.30.N; 05.70.F; 64.60; 64.70; 61.50.K

Keywords: A. Acid potassium sulphate; D. Phase transition; D. Proton conductivity; E. Pressure

1. Introduction

$KHSO_4$ belongs to the class of hydrogen bonded compounds with the general chemical formula $AHBO_4$, where A is a monovalent cation (Cs, Rb, NH_4, K, Na), and B stands for S or Se. A typical structural feature of $AHBO_4$ compounds is the occurrence of $(HBO_4)_2$-dimers and HBO_4^{∞}-chains being separated from each other by A-cations. It is believed that the hydrogen bonding pattern between HSO_4^- tetrahedral ions in the dimers and chains is responsible for the ferroelectric phase transitions in this class of compounds. Members of this type of compounds are known to undergo few reversible and irreversible phase transitions above the room temperature and below the melting point. The amplitude of librational and rotational motions of BO_4 tetrahedra increases with heating, and the $AHBO_4$ framework looses its rigidity allowing protons to occupy additional crystallographic sites [1]. For large cations such as A = Cs, Rb, NH_4 the compounds exhibit superprotonic conductivity in high temperature phases. The transition temperature to the superprotonic state decreases with the increase of the cation size [2]. By doping $CsHSO_4$ with K, the superprotonic phase transition in the system $Cs_{1-x}K_xHSO_4$ vanishes for $x \geq 0.75$ [3]. Note that the crystal structures of $CsHSO_4$ and $KHSO_4$ are different.

The mechanism of proton transport in the high temperature phases consists essentially in a motion of H within a double-well potential and the associated migration of H between two adjacent crystallographic sites. The conductivity in the low temperature phases was suggested to be related to the dynamics of H-bonds inside chains [4]. That is called the Grotthuss mechanism of proton conductivity [5]. At higher temperatures an additional

* Corresponding author. Tel.: +49 69 79823376; fax: +49 69 79823280.
E-mail address: nickbagd@geophysik.uni-frankfurt.de (N. Bagdassarov).

0038-1098/$ - see front matter © 2005 Elsevier Ltd. All rights reserved.
doi:10.1016/j.ssc.2005.06.028

contribution to proton conductivity arises from the synchronous reorientation of H-bonds between dimers and chains in the crystal structure. The role of BO_4^- tetrahedra rotation (or libration) is in the assisting of a break of a double-well H-bond. The activation energy of proton transfer in superprotonic conductor is defined by the energetic barrier within the double-well hydrogen bond and is of the order of ~0.1–0.6 eV [1]. The phase transition in a superprotonic conductor is affected by moisture, pressure and concentration of impurities. During the phase transition, the electrical conductivity jumps to values of 10^{-3}–$10^{-2}\ \Omega^{-1}$/cm, and materials become plastic [6,7]. The typical activation energy of the electrical conductivity in high temperature phases of hydrogen bonded sulphates is 0.3–0.45 eV [7]. The proton conductivity in these compounds does not need a humid atmosphere making these materials attractive for fuel-cell applications. The low temperature non-conductive phase often does not appear upon cooling of the high temperature conductive phase.

$KHSO_4$, also known as the mineral mercallite, crystallizes in the orthorhombic space group $Pbca = D_{2h}^{15}$ [8,9], with two inequivalent H-sites, and a total of 16 formula units per unit cell. The dimensions of the unit cell are $8\times9\times18$ Å^3. As mentioned above, the two different types of HSO_4^- tetrahedra in the asymmetric unit are differently linked by hydrogen bridges: one type forms dimers across a centre of symmetry with O···O distances varying from 2.67 to 2.619 Å; the other type is linked into infinite chains along the *a*-axis with O···O distances varying from 2.67 to 2.573 Å [8]. Due to the chain orientation parallel to the *a*-axis, $KHSO_4$ crystals possess a marked anisotropy of the elastic stiffness ($c_{11}=57$ GPa, $c_{22}\approx c_{33}=31$ GPa) and the thermal expansion coefficients ($\alpha_{11}=5.6\times10^{-6}$, $\alpha_{22}=59\times10^{-6}$, and $\alpha_{33}=68\times10^{-6}\ K^{-1}$) [10]. The length of four S–O bonds in HSO_4^- in early studies has been reported all equal [8], later it was shown that in $KHSO_4$, in the tetrahedral ion SO_4^{2-}, the S–O bonds are 1.44, 1.475 Å long, an S–OH bond is longer, $c=1.57$ Å [9,11,12].

Phase transitions in $KHSO_4$ have been studied by several techniques: TGA, DTA, DSC [13–15], dilatometry [16], NMR [13,17], electrical conductivity measurements [13,17], and in situ X-ray measurements [18]. There is a general consensus about the phase transition at 178 °C [13,14,17], which was earlier interpreted as a superposition of two phase transitions at 164 and 181 °C. The melting point of potassium hydrogen sulphate is still the matter of discussions and has been estimated from 207 °C by electrical conductivity [19] and 208 °C by DSC to 215 °C from electrical conductivity measurements [13]. The phase transition at 120 °C has been identified by DTA [14], electrical conductivity measurements [17] and by in situ X-ray powder diffraction [18]. In Ref. [14] the changes of physical properties in $KHSO_4$ at 120, 178 and 212 °C are interpreted as not related to the structural phase transition, but rather as a result of the water desorbtion (120°) and of the reversible chemical dehydration (178, 212 °C) on the surface of $KHSO_4$ crystals.

A suitable doped potassium hydrogen sulphate crystal is known to be a pure proton conductor [4,20]. Previous conductivity measurements on $KHSO_4$ were performed at ambient pressure and are summarised in Fig. 1. The non-doped crystals of $KHSO_4$ do not show the signature of a superprotonic phase transition. Instead, the differing conductivity values were found at lower temperatures, together with variations in phase transition and melting temperatures.

Contrary to $KHSO_4$, the high temperature tetragonal phases of $RbHSO_4$ and NH_4HSO_4 are known to possess a superprotonic state at high pressures, i.e. a decrease in radius of A in $AHSO_4$ compound is equivalent to a pressure increase (see Ref. [7,23] and references therein). Under the hydrostatic pressure 0.6 and 0.28 GPa $RbHSO_4$ and NH_4HSO_4 become superprotonic conductors, respectively [7]. The question still remains whether K-cation, which is even smaller than Rb or ammonium, also allows the transformation to a high-pressure superprotonic state. Consequently, the temperature dependence of the $KHSO_4$ conductivity at high pressures were studied.

Structural properties of $KHSO_4$ at high pressure are unknown. The only high pressure study published so far concerns the investigation of phase transitions in $KHSO_4$ by Raman-spectroscopy [24]. In the present paper the electrical impedance of polycrystalline $KHSO_4$ has been measured in the temperature interval from 100 to 330 °C at pressures of 0.2, 0.5, 1.5, 2.0 and 2.5 GPa.

2. Experimental

Crystalline powder of $KHSO_4$ was prepared from an aqueous solution of K_2SO_4 and H_2SO_4 at the ratio 1:2 by slow evaporation. The products before and after the high pressure runs were identified by the X-ray powder

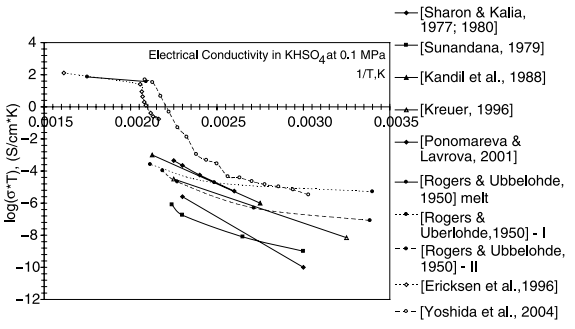

Fig. 1. The electrical conductivity measurements in $KHSO_4$ at 0.1 MPa [2,4,13,16,17,19–22]. The melting point T_m estimated by different authors is: 207 °C [19], 215 °C [13], 205–208 °C [15], 212 °C [14]. The phase transition to the high temperature conductive phase prior to melting has been estimated as 178 °C from electrical conductivity measurements [13].

diffraction. The crystals are slightly hydroscopic and hence, were dried for 24 h at 110 °C prior to the conductivity measurements.

2.1. Electrical conductivity measurements

The measurements of the electrical impedance were performed at pressures up to 1 GPa and temperatures up to 500 °C. The $KHSO_4$ powder was pressed in the coaxial gap between two concentric cylindrical electrodes made from Pt-tubes having 3.8 and 2.2 mm diameters and 0.1 mm thickness. The length of the capacitor varied from 6.5 to 4. 5 mm. The inner part of the high-pressure cell and the pressure calibration procedure are described elsewhere [25].

For each temperature and pressure, the impedance Z over the frequency range 3×10^{-2}–3×10^{5} Hz has been measured. The bulk electrical conductivity of $KHSO_4$ was estimated from Argand plots, the dependence of $-\mathrm{Im}[Z]$ from $\mathrm{Re}[Z]$. The intersection of the $-\mathrm{Im}[Z]$ arc with the $\mathrm{Re}(Z)$ axes defines the bulk resistance of the sample. The frequency scan data can be fitted to a sum of two relaxation functions:

$$Z_p = \frac{R_1}{1+(j\omega\tau_{\mathrm{e.p.}})^p} + \frac{R_2}{1+(j\omega\tau_{\mathrm{d.l.}})^n} \quad (1)$$

where the first term corresponds to the low frequency dispersion, and the second term stands for the dielectric losses in the sample [26] with Z_p is the measured impedance, R_i is the active resistance, j is $\sqrt{-1}$, ω is the frequency, τ_i is the dielectric relaxation time. The temperature dependence of $\tau_{\mathrm{d.l.}}$ determines the activation energy of the dielectric loss peak. The parameter n in Eq. (1) characterises the broadness of the dielectric loss peak in comparison with a Debye peak ($n=1$).

The bulk DC-conductivity σ_{DC} of the sample is calculated from Eq. (1) according to $\sigma_{\mathrm{DC}}=1/(R_1G)$, where G is the geometric factor of the capacitor cell (5–8 cm in this study). The activation energy of the bulk conductivity, E_σ was derived from the Arrhenius equation as follows

$$\sigma_{\mathrm{DC}}T = \sigma_0 \mathrm{e}^{-E_\sigma/(kT)} \quad (2)$$

where T is the temperature in Kelvin, k is the Boltzmann's constant, σ_0 is the pre-exponential factor.

3. Results

The bulk resistance was determined from the Arrhenius plots of the electrical measurements covering the temperature range both below and above the solid phase transitions and the melting of $KHSO_4$. Fig. 2(a)–(c) shows the measurements at 0.5, 1, 1.5, 2, and 2.5 GPa, the first heating and the subsequent cooling and heating cycles. The data are presented in a form of the Arrhenius plot. The change of the slope on the curve evidences the drastic increase of the electric conductivity prior to melting. It is difficult to elaborate a criteria to determine the phase transition and the melting temperatures from $\log(\sigma T)$ vs. $1/T$, K plot. The phase transition in a conductive phase may be identified by a temperature point corresponding to the steep increase of $\log(\sigma T)$ vs. $1/T$, K and to the abrupt change of the activation energy E_σ [13]. In the low temperature phase E_σ is 0.37 eV, above the phase transition temperature E_σ exceeds 2–3 eV. The melt characterises by the activation energy about 0.2 eV. However, in Ref. [17], the phase transition temperature was identified in the middle of the temperature interval, where the steep increase of conductivity occurs, i.e. T_{Tr} relates to a change of the activation energy from 3.3 to 3.9 eV. In the present study, the electrical impedance measurements were realised during heating and cooling with a rate $\sim$1 K/min.

The results of the bulk electrical conductivity measurements for $K_3H(SO_4)_2$ from Ref. [27] are shown in Fig. 2 for comparison. Fig. 2(a) represents three subsequent heating cycles plotted in the Arrhenius diagram. The identification of the melting temperature is straightforward, it corresponds to the activation energy 0.23 eV. The T_{Tr}, the temperature of the α–β phase transition, corresponds to the point of the deviation of the bulk electrical conductivity from the Arrhenius dependence. The cooling and heating cycles follow different paths (Fig. 2(a)), which is due to disordering of the $KHSO_4$ structure above T_{Tr} and in the phase melt. After annealing of the high temperature phase at $T\sim100$ °C over *c.* 1–2 h, the conductivity decreases to the initial value of the low temperature phase. During several successive cycles of heating and cooling, the conductivity data, melting temperature and T_{Tr} were reproducible. Up to 1 GPa T_{Tr} and T_{m} increase with pressure. In experiment at 1 GPa (Fig. 2(b)) the measurements have been done also after the pressure release from 1 to 0.2 GPa. The bulk conductivity data in a depressurised sample indicates the reversible decrease of melting and phase transition temperatures after decompression. The measurements obtained at pressures 1.5, 2 and 2.5 GPa demonstrate a decrease of melting and phase transition temperatures with increasing pressure above 1.5 GPa.

The activation volume calculated from E_{a} which was measured from the data in Fig. 2(a)–(c) is *c.* $+0.2\pm0.1$ cm^3/mol at pressures below 1.5 GPa and is *c.* -0.2 ± 0.1 cm^3/mol at $P>1$–5 GPa. The reported activation volume of the electrical conductivity for $CsHSO_4$ is 0.1–1 cm^3/mol and for NH_4HSO_4 is <2 cm^3/mol [23].

4. Discussion

The pressure dependence of α–β phase transition and melting in $KHSO_4$ may be estimated from Klasius–Clayperon relationship

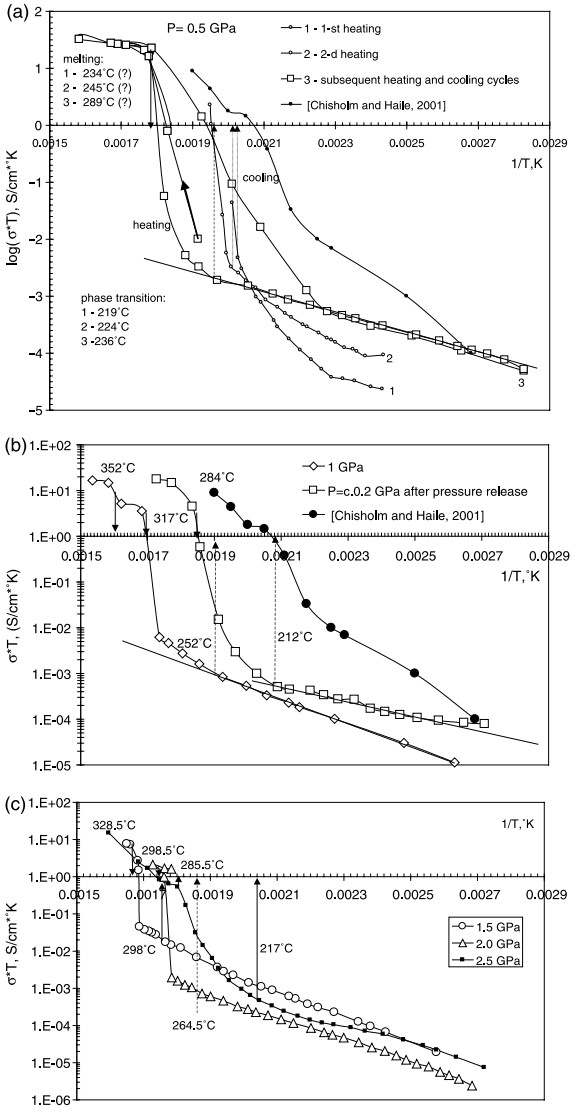

Fig. 2. (a) The electrical conductivity measurements at 0.5 GPa in $KHSO_4$. (1) The first heating to 225 °C characterised by $E_s = 1.61$ eV prior to α–β transition in $KHSO_4$; the phase transition and melting points are 219 and 234 °C, respectively. (2) The second heating to 240 °C characterised by $E_\sigma = 0.77$ eV prior to α–β and higher temperatures of transformation 224 °C and melting 245 °C. The electrical impedance results are affected by the decomposition process of $KHSO_4$. In a decomposed mixture of $KHSO_4$ and $K_3H(SO_4)_2$ melting is characterised by $E_\sigma = 0.23$ eV above 289 °C. The low temperature phase has an activation energy 0.42 eV. These values are in good agreement with the data of [17], where the low temperature phase possesses $E_\sigma = 0.39$ eV, and prior to the α–β transition E_σ changes from 3.2 to 3.9 eV and in the melt E_σ is 0.18 eV. The difference in conductivity during cooling and heating cycles reflects the disordering of $K_3H(SO_4)_2$–$KHSO_4$ structure near the α–β phase transition at 236 °C. The data of the electrical conductivity in $K_3H(SO_4)_2$ from Ref. [27] are shown for comparison. (b) The electrical conductivity measurements in $KHSO_4$ at 1 GPa and after pressure release to *c*. 0.2 GPa. Prior to the temperature of the phase transition E_σ is 0.42 and 0.53 eV, respectively. The data of electrical conductivity in $K_3H(SO_4)_2$ from Ref. [27] are shown for comparison. (c) The electrical conductivity of $KHSO_4$ at 1.5, 2.0 and 2.5 GPa. The arrows indicate the phase transition and melting temperatures. E_a of the electrical conductivity in the high temperature phase is 0.56, 0.42 and 0.23 eV, respectively.

$$\frac{dT}{dP} = \frac{\Delta V}{\Delta S} = \frac{T\Delta V}{\Delta H} \tag{3}$$

where ΔV and ΔH are the changes of specific volume and enthalpy at normal pressure. There are only few measurements of the volume and enthalpy changes of the α–β phase transition in $KHSO_4$. In Ref. [16] the reported $\Delta V/V$ is $\sim +0.12\%$. The measured endothermic ΔH is 2.11 kJ/mol at 178 °C [13,15]. Using the specific volume at 22 °C, 58.83 cm^3/mol, and the volume thermal expansion coefficient, 1.33×10^{-4} K^{-1}, from Ref. [10], the extrapolated ΔV at 178 °C is -0.0725 cm^3/mol and the calculated dT/dP is $\sim +15.5$ K/GPa. For melting, $\Delta V = +2.65$ cm^3/mol or 4% [19], $\Delta H = 16.6$–16.2 kJ/mol [13,15], and the estimated dT/dP is from 77 to 79 K/GPa. The recent determinations of enthalpies for melting (crystallisation) are 14.6 (14.8) kJ/mol at 205 (188 °C) and for the α–β phase transition is 1.63 kJ/mol at 182 °C during heating [28]. These values provide a slope +87 and +20 K/GPa for melting and the α–β phase transition, respectively. This difference in slopes of the pressure dependence of melting and the α–β phase transition means that with the pressure increase the temperature interval of the β-phase stability should be larger before melting occurs. In Ref. [23] the reported pressure dependence of the superprotonic phase transition temperature in $CsHSO_4$ is *c*. 5 K/GPa, and about 0 K/GPa in NH_4HSO_4. In comparison, melting temperatures of $CsHSO_4$ depends much stronger on temperature $dT_m/dP \sim +100$ K/GPa [23], and, thus, the pressure increases the temperature range of the superprotonic phase stability. In contrast, for $A_3H(SO_4)_2$ crystals dT_{Tr}/dP is negative from -40 to -60 K/GPa [7].

Fig. 3 represents the measured temperatures of the α–β phase transition and melting temperatures estimated from electrical conductivity measurements by using $\log(\sigma T)$ vs. $1/T$ plots in Fig. 2(a)–(c). The estimated dT/dP slopes for melting differ significantly from the predicted values. Moreover, above 1.5 GPa the dT/dP slopes become negative. This could be caused by an unknown phase transition or a pressure induced amorphization in potassium hydrogen sulphate. However, the most plausible explanation is the instability of $KHSO_4$ under pressure. The Raman scattering experiments in diamond anvils [24] demonstrated that at $P > 0.4$ GPa the Raman spectrum of $KHSO_4$ evolves in spectrum similar to $K_3H(SO_4)_2$. The suggested decomposition reaction is as follows:

$$3KHSO_4 \leftrightarrow K_3H(SO_4)_2 + H_2SO_4 \tag{4}$$

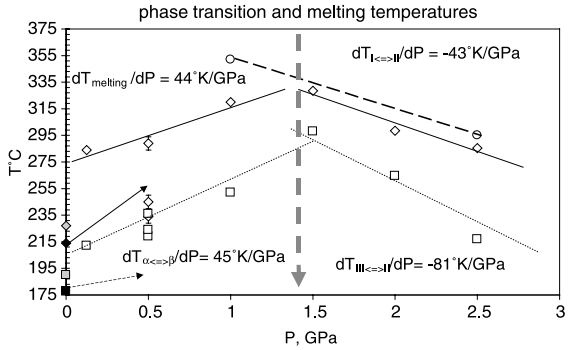

Fig. 3. The results of the melting and T_{Tr} temperature measurements obtained by the electrical impedance measurements. The melting point and T_{Tr} at 0.1 MPa are from Ref. [13] black filled symbols, measured by the differential enthalpic analysis. The grey filled symbols are phase transition temperatures in $K_3H(SO_4)_2$ from Ref. [27]. Above the turnover point 1.5 GPa, the negative slopes of dT/dP indicate probably a decomposition of $KHSO_4$. The arrows indicate the calculated slope dT/dP for melting and α–β phase transition in $KHSO_4$. The vertical trend of points at 0.5 GPa is probably a result of the progressive decomposition of $KHSO_4$ into $K_3H(SO_4)_2$.

The results of the electrical conductivity measurements obtained at 0.5 GPa (Fig. 2(a)) clearly demonstrate the change of physical properties of the starting composition after few successive heating–cooling cycles. The decrease of the activation energy and the increase of the characteristic points on the curves $\log(\sigma T)$ vs. $1/T$, K evidence the progressive increase of the $K_3H(SO_4)_2$ content in the starting $KHSO_4$ composition. The comparison of the measured $\log(\sigma T)$ vs. $1/T$, K curves at pressures and the results for $K_3H(SO_4)_2$ in Ref. [27] suggests a certain similarity of the electrical conductivity behavior vs. T (Fig. 2(a)–(c)). Clearly, this similarity is noticeable at 1.0 GPa. At atmosphere pressure, $K_3H(SO_4)_2$ undergoes several phase transitions prior to melting point. During subsequent heating–cooling cycles the transition temperatures may decrease from 227 and 190 to 223 and 185 °C, respectively [27]. DSC study of $K_3H(SO_4)_2$ indicates a dehydration reaction at 206 °C and melting at 269 °C [29].

In a mixture of the $K_3H(SO_4)_2$ and $KHSO_4$ compositions, the characteristic temperatures on the Arrhenius plots may be located between those for $K_3H(SO_4)_2$ and $KHSO_4$. The reason for the negative slope of phase transition temperatures in Fig. 3 above 1.5 GPa is a result of the pressure dependence of the volume difference, i.e. bulk modulus, between parent phase $KHSO_4$ and the decomposition daughter phases: $K_3H(SO_4)_2$ and H_2SO_4 [24]. In general, the turnover of decomposition curve in P–T diagram results from the change of the densities between parent and daughter phases with the increasing pressure. For example, in brucite $Mg(OH)_2$, the turnover pressure of the dehydration reaction is 10 GPa [30].

The XRD of quenched samples indicated clearly on a reversible character of the decomposition reaction. The XRD of samples quenched at 0.5 and 2.5 GPa and 100 °C are identical to the XRD of a starting sample and a standard XRD of mercallite. Only in the quenched sample at 2.5 GPa and 320 °C there are small features (<1%) of XRD of $K_5H_3(SO_4)_4$ (PDF 17-0597 from the ICDD data bank PDF-2), small peaks at $2\theta = 24.5$, 31.8 and 42.5° were observed. This may also suggest a possible decomposition reaction $5KHSO_4 \leftrightarrow K_5H_3(SO_4)_4 + H_2SO_4$, but there are no reliable PDF data to confirm this. In any case, the decomposition reaction of mercallite at high pressure seems to be almost reversible.

5. Conclusions

1. $KHSO_4$ starts to decompose into $K_3H(SO_4)_2$ (and possibly in $K_5H_3(SO_4)_4$) at pressure above 0.5 GPa. The turnover point of the decomposition reaction on P–T diagram is 1.5 GPa. According to XRD of quenched samples this decomposition reaction is reversible.
2. With the pressure increase up to 1.5 GPa the pressure dependencies of T_{Tr} and T_m are positive, having dT/d$P \sim +45$ K/GPa. Above the pressure 1.5 GPa the pressure dependencies of T_{Tr} and T_m are negative, having dT/d$P \sim -45$ K/GPa.
3. The high temperature phase measured in experiments under pressure, presumably a mixture of $KHSO_4$ with $K_3H(SO_4)_2$ and, probably, $K_5H_3(SO_4)_4$, possesses a typical values of the protonic electrical conductivity c. 10^{-1} S/cm up to 2.5 GPa.

Acknowledgements

This research was funded by the German Science Foundation DFG under contract Kn 507/3-1.

References

[1] B.V. Merinov, Solid State Ionics 84 (1996) 89.
[2] K.-D. Kreuer, Chem. Mater. 8 (1996) 610.
[3] T. Mhiri, A. Daoud, Ph. Colomban, Solid State Ionics 44 (1991) 215.
[4] M. Sharon, M. A, K. Kalia, J. Solid State Chem. 31 (1980) 295.
[5] C.J.T. de Grotthuss, Ann. Chim. 58 (1806) 54.
[6] S.M. Haile, D.A. Boysen, G.R.I. Chisholm, R.B. Merle, Nature 410 (2001) 910.
[7] A.I. Baranov, Crystallogr. Rep. 48 (2003) 1012.
[8] L.H. Loopstra, C.H. MacGillavry, Acta Crystallogr. 11 (1958) 349.
[9] F. Payan, R. Haser, Acta Crystallogr. B32 (1976) 1875.
[10] D. Gerlich, H. Siegert, Acta Crystallogr. A 31 (1975) 207.

[11] F.A. Cotton, B.A. Frenz, D.L. Hunter, Acta Crystallogr. B31 (1975) 302.
[12] K. Fukushima, M. Murofushi, M. Oki, K. Igarashi, L. Mochinaga, Y. Iwadate, Z. Naturforsch. 49a (1994) 785.
[13] K.M. Eriksen, R. Fehrmann, G. Hatem, M. Gaune-Escard, O. B. Lapina, V.M. Mastikhin, J. Phys. Chem. 100 (1996) 10771.
[14] J.E. Diosa, R.A. Vargas, E. Mina, E. Torijano, B.-E. Mellander, Phys. Status Solidi B 220 (2000) 641.
[15] G. Hatem, K.M. Eriksen, R. Fehrmann, J. Therm. Anal. Calorim. 68 (2002) 25.
[16] S.H. Kandil, M.E. Kassem, N. El-Rehim Abd, A.M. Bayoumi, Thermochim. Acta 132 (1988) 1.
[17] Y. Yoshida, Y. Matsuo, S. Ikehata, Ferroelectrics 302 (2004) 85.
[18] G. Lentz, K. Knorr, W. Depmeier, C. Baehtz, M. Knapp, W. Morgenroth, Annual Report on HASYLAB, Hamburg, 2001, Part 1.
[19] S. Rogers, A.R. Ubbelohde, Trans. Faraday Soc. 46 (1950) 1051.
[20] C.S. Sunandana, J. Mater. Sci. 14 (1979) 757.
[21] M. Sharon, M. A, K. Kalia, J. Chem. Phys. 66 (1977) 3051.
[22] V.G. Ponomareva, G.V. Lavrova, Solid State Ionics 145 (2001) 197.
[23] A.I. Baranov, E.G. Ponyatovskii, V.V. Synitsyn, R.M. Fedosyuk, L.A. Shuvalov, Sov. Phys. Crystallogr. 30 (1985) 653.
[24] A.K. Arora, T. Sakuntala, High Pressure Res. 17 (2000) 1.
[25] N. Bagdassarov, H. Freiheit, A. Putnis, Solid State Ionics 143 (2001) 285.
[26] A.K. Jonscher, J. Phys. D: Appl. Phys. 32 (1999) R57.
[27] C.R.I. Chisholm, S.M. Haile, Solid State Ionics 145 (2001) 179.
[28] J. Plocek, D. NiŽňanský, P. Vaněk, Z. Mička, J. Sol–Gel Sci. Technol. 28 (2003) 185.
[29] R.H. Chen, R.Y. Chang, C.S. Shern, T. Fikami, J. Phys. Chem. Solids 64 (2003) 553.
[30] Y. Fei, H.-k. Mao, J. Geophys. Res. 98 (1993) 11875.